

Smart Aptamers Facilitate Multi-Probe Affinity Analysis of Proteins with Ultra-Wide Dynamic Range of Measured Concentrations

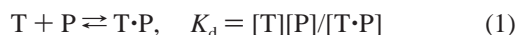
Andrei P. Drabovich, Victor Okhonin, Maxim Berezovski, and Sergey N. Krylov*

Department of Chemistry, York University, Toronto, Ontario M3J 1P3, Canada

Received April 1, 2007; E-mail: skrylov@yorku.ca

Protein concentrations can vary over several orders of magnitude in many physiological and pathological processes.¹ Studies of these processes require affinity analysis of proteins with a very wide dynamic range of accurately measured concentrations. Such an analysis can be realized with multiple affinity probes that bind the target with significantly different equilibrium constants (K_d).² Every probe in a multi-probe affinity analysis is responsible for detection of the target in the range of concentrations around its K_d value. A multi-probe affinity analysis of proteins was out of practical reach due to the lack of high-selectivity affinity probes with a wide range of K_d values.³ Kinetic capillary electrophoresis (KCE) has been recently proven to generate “smart” DNA aptamers with high selectivity and a wide range of predefined K_d values.⁴ Here, we demonstrate that such aptamers can facilitate multi-probe affinity analysis of a protein with an ultra-wide dynamic range of measured concentrations. In this proof-of-principle work, we used smart aptamers for MutS protein with K_d values of 7.6, 46, and 810 nM. MutS protein is an important and intensively studied player of the DNA repair machinery. Our results showed that the three-aptamer analysis of MutS had a concentration dynamic range of more than 4 orders of magnitude with an accuracy of 11%. To the best of our knowledge, this is the widest dynamic range ever reported for affinity analyses of proteins. This work proves that the wide range of predefined binding parameters of smart aptamers can bring new capabilities to quantitative affinity analyses. The same feature of smart aptamers makes them potentially indispensable molecular tools in studies of intracellular processes.

In a generic affinity analysis, a spectroscopically visible affinity probe P of known concentration $[P]_0$ is reacted with a spectroscopically invisible target T of unknown concentration $[T]_0$, which is to be determined. P binds T and forms a detectable target–probe complex T·P at equilibrium



where $[T]$, $[P]$, and $[T \cdot P]$ are equilibrium concentrations of T, P, and T·P, respectively. The free probe is separated from the target–probe complex physically or spectrally to find fraction f of the bound probe in the equilibrium mixture: $f = [T \cdot P]/[P]_0$. Finally, the unknown concentration of target is calculated

$$[T]_0 = ([P]_0 + K_d/(1 - f))f \quad (2)$$

In a general case, when a mixture of n ($n \geq 1$) probes is used, eq 2 converts into the following (see Supporting Information):

$$\sum_{i=1}^n \frac{[P]_{0i}}{K_{di} + [T]_0 - f \sum_{j=1}^n [P]_{0j}} = \frac{f \sum_{i=1}^n [P]_{0i}}{[T]_0 - f \sum_{i=1}^n [P]_{0i}} \quad (3)$$

where K_{di} and $[P]_{0i}$ are the parameters of probe i ($i = 1, \dots, n$).

Binding curves f versus $[T]_0$, which are obtained from eq 3, visualize the dynamic range of the analysis (Figure 1). The concentration dynamic range is the region of $[T]_0$ where the binding curve has a slope sufficiently steep to find $[T]_0$ with a required accuracy. When a single probe is used in an affinity analysis, the dynamic range lies around its K_d value and typically covers only 1–2 orders of magnitude. The dynamic range can be greatly extended if more than one probe with significantly different K_d values is used (Figure 1). The probes can be used individually in separate analyses to achieve the greatest extension (Figure 1A). Alternatively, they can be used as a mixture in a single analysis with still a very wide dynamic range and an advantage of simplicity (Figure 1B). To have a dynamic range of 4 orders of magnitude, the multi-probe analysis has to employ affinity probes with K_d values in a range of at least 2 orders of magnitude (the difference in K_d between “adjacent” probes should not significantly exceed 1 order of magnitude to avoid blind areas on the binding curve; see Supporting Information). Obtaining antibodies with a K_d range of 2 orders of magnitude is virtually impossible without compromising their selectivity. We have recently proven that DNA aptamers provide a vital alternative.⁴

Aptamers are selected in a process termed SELEX.⁵ The conventional SELEX typically requires more than 10 rounds of selection and leads to very few unique aptamers with binding parameters in a narrow and hardly predictable range. Selection of smart aptamers by methods of KCE overcomes the limitations of conventional SELEX: the number of required rounds is typically below five, and a large number of unique aptamers can be selected with binding parameters predefined in a wide range.⁴

In our recent work, we used KCE to select smart DNA aptamers for MutS protein with predefined K_d values in a range of over 2 orders of magnitude.^{4b,c} Here we employed three of those aptamers with K_d values of 7.6, 46, and 810 nM to develop the first aptamer-based multi-probe affinity analysis. The generic procedure for an affinity analysis described above was used with the following specifics. The aptamers were fluorescently labeled for sensitive detection. The individual aptamers or an equimolar mixture of them was reacted with MutS to reach equilibrium. The aptamer–protein complexes were separated from free aptamers by a KCE method known as nonequilibrium capillary electrophoresis of equilibrium mixtures (NECEEM).⁶ The fraction of the bound aptamer was calculated from the areas of peaks in a NECEEM electropherogram as explained in Figure 2.

Using this approach, we built binding curves f versus $[T]_0$ for the three individual aptamers (Figure 3A) and for their equimolar mixture (Figure 3B). All experiments were done in triplicate, and their results are shown as points. Theoretical binding curves were calculated using eq 3; they are shown as solid lines. Importantly, the theoretical curves fit perfectly the experimental data. This suggests that aptamers bind MutS with 1:1 stoichiometry, and no

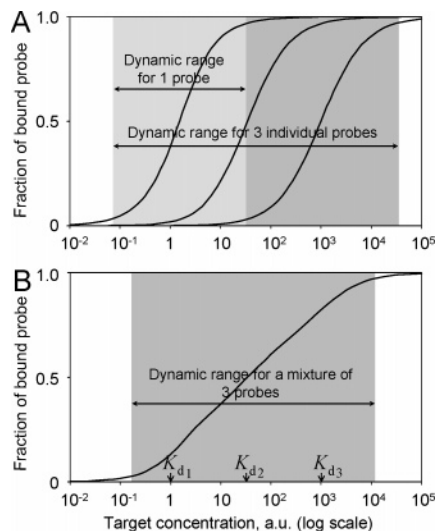


Figure 1. Schematic representation of the dynamic range extension for affinity analysis using three individual affinity probes with K_d values of 1, 33, and 1000 au and a concentration of 1 au (A) and a mixture of these probes at concentrations of 1 au each (B). The binding curves were calculated using eq 3 with $n = 1$ (panel A) and $n = 3$ (panel B).

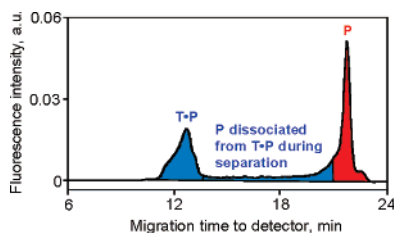


Figure 2. Determination of the fraction f of bound aptamer in aptamer-based affinity analysis of MutS protein using the NECEEM method. The blue and red areas in the electropherogram represent the amounts of bound and unbound aptamer, respectively, in the equilibrium mixture. The fraction of bound aptamer is calculated as a ratio between the blue and the sum of the blue and red areas corrected for migration times of corresponding species (see Supporting Information).

interference occurs between the aptamers in the mixture. It also suggests that building the calibration curves for the affinity analysis is not necessary; eq 3 can be directly utilized for finding unknown $[T]_0$ using known K_d , f , and $[P]_0$. The concentration dynamic ranges for affinity analyses were defined for 11% accuracy of protein concentration determination. The dynamic range for a single-probe analysis was approximately 2 orders of magnitude. The three individual probes covered the overall dynamic range of 5 orders of magnitude. The analysis based on a mixture of the three probes had a dynamic range of more than 4 orders of magnitude with a limit of detection of 0.1 nM of $[MutS]_0$. These results prove that smart aptamers can facilitate multi-probe affinity analysis of proteins with an ultra-wide dynamic range. Moreover, the three-aptamer analysis of MutS developed here can be directly used in studying cellular DNA repair machinery.

We then tested the selectivity of the aptamer-based multi-probe affinity analysis of MutS. Different concentrations of MutS (0.18 μ g to 0.18 mg in mL) were detected in the presence of 2.5% fetal bovine serum (FBS), which contained 1.1 mg/mL of total protein. MutS in the presence of FBS was measured using the mixture of the three aptamers. The results of such analyses (Figure 3B, black squares) showed no significant difference from those of the analyses of MutS in a bare buffer. The tolerance of the analysis to the presence of other proteins suggests its potential utility in applications ranging from basic research to clinical analyses.

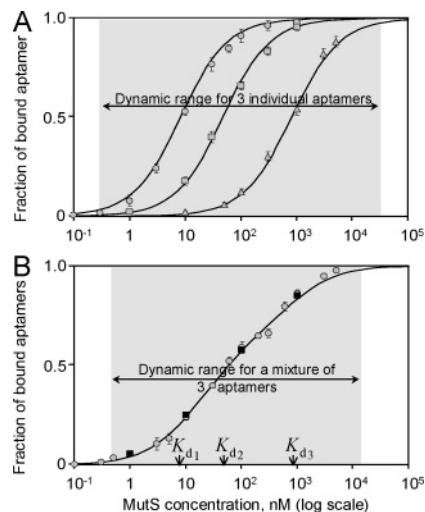


Figure 3. Concentration dynamic range for the affinity analysis of MutS protein using 1 nM of three individual aptamers with K_d values of 7.6, 46, and 810 nM (A), and a mixture of 1 nM of these aptamers (B). Solid lines were calculated with eq 3 using the above values of K_d and concentrations. Gray points correspond to analyses of MutS in the bare buffer (50 mM Tris-acetate, pH 8.2), while black squares correspond to analyses of MutS in the presence of 2.5% FBS in the buffer.

Finally, we outline the major features of the multi-aptamer affinity analysis of protein. The use of multiple aptamers extends the concentration dynamic range to more than 2 orders of magnitude plus the range of K_d values of the aptamers used. Advantageously, the concentration of the target can be found with a simple calibration-free approach. When the target is present in a complex biological matrix, protecting aptamers from nucleases can be required. If the sample matrix contains DNA-binding proteins, their nonspecific binding to aptamers can be suppressed by adding the excess of nonlabeled scrambled DNA.

To conclude, this work proves that unique features of smart ligands can significantly extend capabilities of quantitative affinity analyses. The particular analysis developed here is being productively used in studies of MutS protein, an important player in the DNA repair machinery. We foresee new enabling applications of smart ligands in analyses and therapies that require well-defined dynamics of target–ligand interaction.

Acknowledgment. The work was funded by NSERC Canada.

Supporting Information Available: Supporting materials and methods and complete ref 3 (PDF). This material is available free of charge via the Internet at <http://pubs.acs.org>.

References

- (1) (a) Moll, D.; Prinz, A.; Gesellchen, F.; Drewianka, S.; Zimmermann, B.; Herberg, F. W. *J. Neural Transm.* **2006**, *113*, 1015–1032. (b) Wilson, D. W. *Science* **2002**, *295*, 2103–2105. (c) Yamaguchi, H.; Yoshida, J.; Yamamoto, K.; Sakata, Y.; Mano, T.; Akehi, N.; Hori, M.; Lim, Y.-J.; Mishima, M.; Masuyama, T. *J. Am. Coll. Cardiol.* **2004**, *43*, 55–60.
- (2) Marvin, J. S.; Corcoran, E. E.; Hattangadi, N. A.; Zhang, J. V.; Gere, S. A.; Hellinga, H. W. *Proc. Natl. Acad. Sci. U.S.A.* **1997**, *94*, 4366–4371.
- (3) Taussig, M. J.; et al. *Nat. Methods* **2007**, *4*, 13–17.
- (4) (a) Petrov, A.; Okhonin, V.; Berezovski, M.; Krylov, S. N. *J. Am. Chem. Soc.* **2005**, *127*, 17104–17110. (b) Drabovich, A.; Berezovski, M.; Krylov, S. N. *J. Am. Chem. Soc.* **2005**, *127*, 11224–11225. (c) Drabovich, A. P.; Berezovski, M.; Okhonin, V.; Krylov, S. N. *Anal. Chem.* **2006**, *78*, 3171–3178. (d) Berezovski, M.; Musheev, M.; Drabovich, A.; Krylov, S. N. *J. Am. Chem. Soc.* **2006**, *128*, 1410–1411. (e) Berezovski, M.; Musheev, M. U.; Drabovich, A. P.; Jitkova, J.; Krylov, S. N. *Nat. Protoc.* **2006**, *1*, 1359–1369.
- (5) (a) Tuerk, C.; Gold, L. *Science* **1990**, *249*, 505–510. (b) Mendonsa, S. D.; Bowser, M. T. *J. Am. Chem. Soc.* **2004**, *126*, 20–21.
- (6) Berezovski, M.; Krylov, S. N. *J. Am. Chem. Soc.* **2002**, *124*, 13674–13675.

JA072269P